Geophysical Research Letters

RESEARCH LETTER
10.1029/2019GL085602

Key Points:
- Polar diatom biomass derived from temperate allometry can lead to systematically low estimates
- Diatoms' contributed a majority to POC standing stock and export during the JGOFS AESOPS program (original estimates <20%)
- Increasing SST in polar regions will likely reduce diatom elemental density and alter the flow of organic matter to higher trophic levels

Supporting Information:
- Supporting Information S1

Correspondence to:
J. W. Krause,
jkrause@disl.edu

Citation:
Krause, J. W., & Lomas, M. W. (2020). Understanding diatoms' past and future biogeochemical role in high-latitude seas. *Geophysical Research Letters*, *47*, e2019GL085602. https://doi.org/10.1029/2019GL085602

Received 27 SEP 2019
Accepted 18 DEC 2019
Accepted article online 23 DEC 2019

Understanding Diatoms' Past and Future Biogeochemical Role in High-Latitude Seas

Jeffrey W. Krause[1,2] and Michael W. Lomas[3]

[1]Dauphin Island Sea Lab, Dauphin Island, AL, USA, [2]Department of Marine Sciences, University of South Alabama, Mobile, AL, USA, [3]Bigelow Laboratory for Ocean Sciences, East Boothbay, ME, USA

Abstract Because cold-water diatoms' baseline elemental density (BED) is substantially higher than temperate diatoms, previous polar studies may have underestimated diatoms' contribution to elemental standing stocks, contribution to particulate organic carbon (POC) export and incorrectly modeled their susceptibility to future warming. We apply cold-water diatom allometry to Arctic field samples and derive diatom growth rates ranging from 0.01–0.68 day^{-1}, versus unrealistically high rates estimated using temperate diatom allometry. Reanalysis of published Southern Ocean data (Antarctic Environment and Southern Ocean Process Study and European Iron Fertilization Experiment) shows that diatom POC was significantly underestimated and diatoms could have accounted for a majority of POC export. However, during some field programs (Kerguelen Plateau), temperate allometry properly accounted for diatom biomass. We also predict that warming sea surface temperature may alter high-latitude diatom BED, suggesting that even if abundances do not change with warming, the reduced diatom BED will likely lower the trophic-transfer efficiency and their total carbon flow to consumers.

Plain Language Summary High-latitude marine regions are warming faster than other marine systems. We show that the role of diatoms in these systems, already thought to be important, was systematically underestimated in some studies due to insufficient understanding of cold-water diatoms' physiology, specifically their high elemental density. When applying cold-water-diatom elemental density relationships to original and previously published high-latitude field data, diatom growth rates were rapid (up to a doubling per day), and they could account for most of the organic carbon standing stock and its export—original publications inferred contributions <20%. We predict that cold-water diatom elemental density will decline with increasing warming. Such a decline in diatom food quality (less element per volume), even without diatom abundance declines, may reduce transfer of their material to consumers and affect food webs.

1. Introduction

Diatoms often dominate primary production and phytoplankton biomass during blooms in high-latitude marine environments (Assmy et al., 2013; Brzezinski et al., 2001). While many diatom blooms in these regions are short lived (e.g., weeks), they can account for disproportionately high quantities of annual primary production and regulate the capacity for these ecosystems to take up atmospheric CO_2 (Tremblay et al., 2002).

Accurately determining diatom-specific carbon fluxes in polar systems requires quantifying both their growth rate and contribution to carbon standing stock. Silicon tracers have the potential to resolve diatom growth rates, as diatoms are the only major phytoplankton group having an obligate requirement for silicon. Diatoms typically dominate the biogenic silica ($bSiO_2$) standing stock and silicon uptake in high-latitude seas, but silicon tracer methods have a bias when used to derive growth rates. The $bSiO_2$ production rates (Si volume^{-1} time^{-1}) normalized to $bSiO_2$ (Si volume^{-1}) result in growth estimates (time^{-1}) which are systematically underestimated when any nonliving $bSiO_2$ is present. This highlights a broader challenge of determining any phytoplankton groups' contribution to elemental standing stock.

To alleviate the problem of disentangling components in bulk particulate samples, microscopy analysis (cell abundance and biovolume) can be used to quantify living cell proportions of bulk measurements. Diatom biovolume, without bias from detritus or other phytoplankton cells, can be converted to elemental

content using allometry. This approach is powerful, and when combined with diatom growth rates, the community has been able to infer diatom contributions to carbon flow (Brown & Landry, 2001; Selph et al., 2001). Allometry also enables information on variability of diatom standing stocks at regional (Sherr et al., 2003) or global scales (Leblanc et al., 2012).

Recent laboratory work demonstrates that cold-water diatom allometry is unique (Lomas et al., 2019). While both cold-water adapted and temperate/tropical (hereafter "temperate") diatoms increase their elemental content with increasing biovolume at a similar rate, the baseline elemental density (BED) is substantially higher in polar diatoms for C, N, P, and Si. Therefore, the element amount per unit volume (μm^3) for cold-water adapted diatoms will be higher than for temperate diatoms across all biovolume ranges. The implication for this finding is that previous polar studies applying temperate allometric relationships to quantify diatom standing stocks could have systematically underestimated their contribution. This bias affects interpretations of diatoms' contribution to phytoplankton biomass, the underlying mechanisms which promote efficient particulate organic carbon (POC) export, and how diatom processes will be modeled in future warming scenarios. We hypothesize that prior polar studies (Assmy et al., 2013; Brown & Landry, 2001; Lasbleiz et al., 2016) underestimated diatoms' contribution to elemental standing stocks and, consequently, underestimated their role in community processes.

Here we examine a new data set of diatom biomass and production from the Arctic and apply cold-water diatom allometry to derive growth rates. We then reanalyze publicly available data, using this cold-water allometry and revise diatoms' contribution to POC stocks and export upward during two studies in the Southern Ocean; however, prior studies in the Kerguelen Plateau, using temperate allometry, properly accounted for diatom biomass. Finally, we use the BED from cold-water and temperate diatoms to predict how warming sea surface temperature (SST) in high latitudes may alter the food web. This analysis suggests that even if diatom abundance does not change with warming SST, the efficiency of trophic transfer and total carbon flow from diatoms to primary consumers may decline and potentially affect food web dynamics.

2. Materials and Methods

2.1. Study Region, Sample Collection, and Analysis (Original Data)

Cold-water diatom allometric relationships were applied to samples collected at 14 stations during the Arctic Shelf Growth, Advection, Respiration and Deposition (ASGARD) cruise in the northern Bering and Chukchi Seas aboard the R/V Sikuliaq in June 2017 (Table S1 in the supporting information). Water was collected based on the irradiance relative to that just below the surface (%I_0), typically the 50%I_0 depth and the deeper euphotic zone (<5%I_0).

Water was prefiltered through a 200-μm Nitex mesh into a darkened acid-cleaned carboy and subsampled. Triplicate subsamples per depth were taken to measure both $bSiO_2$ standing stock and its rate of production. For $bSiO_2$ standing stock, 0.6–1.0 L was filtered through a 1.2-μm pore size polycarbonate filter. On shore, $bSiO_2$ was quantified using an alkaline digestion in Teflon tubes (Krause et al., 2009). For quantifying $bSiO_2$ production rates, 150-ml polycarbonate bottles were filled, spiked with $^{32}Si(OH)_4$ (367 Bq, >20 kBq μg Si^{-1}), sealed, placed in bags to simulate the %I_0, and incubated in an acrylic deck-board incubator. After a 24-hr incubation, samples were filtered (1.2-μm pore), processed, and ^{32}Si activity was quantified as described elsewhere (Krause et al., 2011). Diatom abundance (single 10-ml subsample per depth) was quantified on a VS Series benchtop FlowCam (Fluid Imaging Technologies; Scarborough, ME) run with no fixatives in autoimage mode (10X objective, 200-μm flow cell); samples were analyzed <2 hr post hydrocast. Diatom images (empty frustules excluded) were manually classified and biovolume (BV, cylinder shape) was automatically measured by FlowCam's image analysis software. The FlowCam software can image chains, but it assigns a single biovolume value; therefore, this analysis is conservative (Figure S2).

Diatom biovolume was converted to $bSiO_2$ standing stock using the cold-water diatom allometric equation: $Log_{10}Si(pmol/cell) = 0.72\ (Log_{10}BV,\ \mu m^3) - 1.34$ (Lomas et al., 2019). This relationship (and that for C, below) were derived from 11 diatom cultures grown at 2 °C. Some clones were originally isolated outside of the polar latitudes (40–59°N) when ambient temperature was ≤3 °C; hence, we use "cold adapted" to

describe the Lomas et al. (2019) allometric equations. The derived $bSiO_2$ associated with the living diatoms was normalized to gross $^{32}Si(OH)_4$ uptake rates to estimate diatom growth rates. Diatom growth rates were comparable to previous literature (Figure S1 and Table S2).

2.2. Ocean Reanalysis

The cold-water diatom allometry was employed during a reanalysis of Southern Ocean data. The U.S. JGOFS Antarctic Environment and Southern Ocean Process Study (AESOPS) project was chosen due to it having four cruises with concurrent POC (Smith et al., 2000), $bSiO_2$ cycling (Brzezinski et al., 2001), biovolume-derived diatom carbon, abundances (Brown & Landry, 2001), and particulate export (Buesseler et al., 2001). Diatom carbon and abundances (L^{-1}) were converted to average diatom C $cell^{-1}$. Then average diatom biovolume $cell^{-1}$ was calculated using the Eppley et al. (1970) equation as reported in Brown and Landry (2001) ($\log_{10}C(pg\ cell^{-1}) = 0.76\ (\log_{10}BV) - 0.352$). These biovolumes were reconverted to diatom POC using the cold-water equation for diatom C versus biovolume in stationary growth ($\log_{10}C) = 0.84(\log_{10}BV) + 0.10$ (Lomas et al., 2019). Live-diatom $bSiO_2$ was calculated using these back-calculated biovolumes with the equation for Si (described above) and using Si allometry in temperate diatoms (Conley et al., 1989). Because all samples (microscopy, POC, $bSiO_2$) were not collected from the same hydrocasts, station averages were calculated for diatom carbon, live-diatom $bSiO_2$, total POC, and total $bSiO_2$ within the upper 50 m. The cold-water diatom allometry (Lomas et al., 2019) was conducted in iron-replete culture conditions. Takeda (1998) reported PON, POP, and BV for two Antarctic diatoms grown in iron-replete and iron-limited culture conditions. PON/P:BV ratios were calculated, and iron-limited diatoms had, on average, 86% of the PON/P:BV of iron-replete diatoms; we applied this reduction factor (0.86) to our reanalyzed diatom POC content to account for iron limitation during AESOPS.

Steady-state Thorium-based export rates were used for this reanalysis (Buesseler et al., 2001). To determine the contribution of diatoms to POC export, the corresponding $bSiO_2$ export was divided by the ratio of water-column $bSiO_2$:diatom carbon, calculated as described above. As discussed previously (Krause et al., 2015), diatoms may be exported from the euphotic zone as intact cells, within fecal pellets or associated with aggregates. Previous studies have estimated diatom contribution to POC export using Si:C ratios for nutrient-replete diatoms, which ignores how diatom material is modified in the food web prior to being exported; hence, the $bSiO_2$:diatom C in the water column is used here. This assumes diatom particulate material is well-mixed within the euphotic zone from grazing and aggregation/disaggregation, with all this material having a similar likelihood to be exported by the aforementioned pathways. Reanalysis data are provided in Table S3.

2.3. Modeling Future Change to Diatom BED With Increasing SST

To predict how diatom carbon BED may change in warming polar seas, we modified the empirical Q_{10} approach described by Eppley (1972)—that is, maximum phytoplankton growth rate versus temperature. Given that elemental content and biovolume relationships vary logarithmically and that we only have diatom carbon BED data for two thermal conditions (temperate, cold-water), we calculated a Q_{10} for BED as a function of SST:

$$(\text{Temperate BED} \times \text{Cold-water BED})^{10*(\text{Temperate SST} - \text{Cold-water SST})}$$

where temperate (10–21 °C) diatom carbon BED is from Menden-Deuer and Lessard (2000) and references therein, and cold-water (2 °C) diatom carbon BED from Lomas et al. (2019). Using this derived Q_{10} metric for diatom carbon BED, we can predict changes to cold-water diatom carbon BED as temperature increases. For the cold-water diatom allometry study, diatom carbon BED were reported for both exponential and stationary growth diatoms, enabling two derived Q_{10} values for BED. Varying the temperature range for each empirical Q_{10} metric provides a range of potential changes to cold-water diatom carbon BED using the Intergovernmental Panel on Climate Change (IPCC) scenarios (IPCC, 2014). In the Arctic Ocean, the SST by the end of the century are predicted to warm by 2–5 and 7–11 °C for RCP2.6 and RCP8.5 scenarios, respectively. These two scenarios are used to predict the trajectory of diatom carbon BED in a warmer ocean.

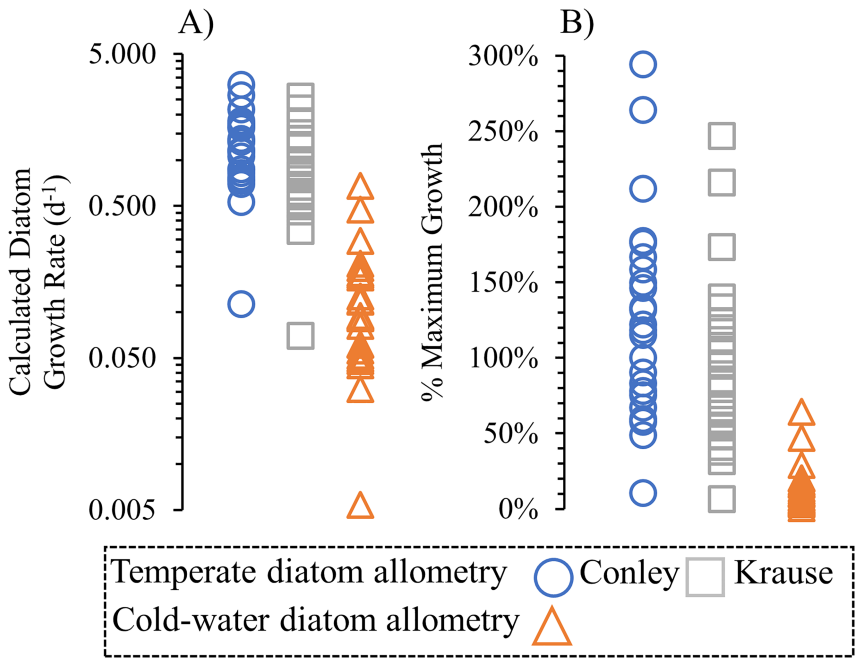

Figure 1. A sensitivity analysis for calculated growth rates using diatom biogenic silica per biovolume estimates for temperate diatoms (circles (Conley et al., 1989); squares (Krause et al., 2010)) versus cold-water diatoms (Lomas et al., 2019). Diatom biovolume was measured using FlowCam, converted to biogenic silica, and then this living-diatom-associated biogenic silica was normalized to gross biogenic silica production. B comparison of calculated growth rate relative to the physiological maximum at the temperature when sampled (Eppley, 1972).

3. Results and Discussion

3.1. "Pumped" up Diatoms in the Polar Environments

Cold-water and temperate diatom allometry were applied to quantify diatom growth rates during ASGARD. The resulting diatom growth rates using temperate diatom allometry (Conley et al., 1989; Krause et al., 2010) were exceptionally high, and in some cases, physiologically impossible based on the water temperature at the time of sampling (−1.2–6.5 °C). Maximum growth rate estimates for each relationship were up to 2.6 and 3.1 day^{-1} (Figure 1(a)), inferring doubling times of 5–6 hr (i.e., greater than four doublings per day), and median values were 0.8 and 1.2 day^{-1} (Figure 1(a)). When cold-water diatom allometry was used to calculate diatom biomass, the resulting growth rate range was 0.01–0.68 day^{-1} (median 0.09 day^{-1}, Figure 1 (a)), inferring a maximum growth rate up to approximately one doubling per day. All calculated growth rates were normalized to the maximum growth rate based on the temperature at the time of sampling (Eppley, 1972). Growth rates derived using the temperate diatom allometry suggested that some diatom assemblages were growing up to 250–300% of their maximum rate with median values at 120% (Conley allometry) and 84% (Krause allometry) of maximum growth. Cold-water-diatom allometry reduced this range, and the maximum rate in the field was only 64% (median 10%) of the maximum theoretical growth rate (Figure 1(b)). Recent work, using metabolic theory (Kremer et al., 2017) shows that the Eppley (1972) relationship overestimates the temperature effect on phytoplankton growth. Therefore, the differences reported here are conservative (Eppley-based maximum growth rate in the denominator is biased high), as mechanistic temperature-growth models would predict an even greater disparity between the calculated temperate allometry growth rates relative to the maximum growth rates inferred from temperature.

The reported lower growth rates, which do not exceed rates predicted by temperature-growth relationships, offer an independent validation of the robustness for the cold-water diatom allometric relationships (Lomas et al., 2019). However, given the widespread use of temperate phytoplankton allometry when estimating diatom contribution to POC in polar environments (e.g., Assmy et al., 2013; Brown & Landry, 2001; Leblanc et al., 2012), these results could have broader consequences to how the community has interpreted diatoms' importance in high-latitude marine systems.

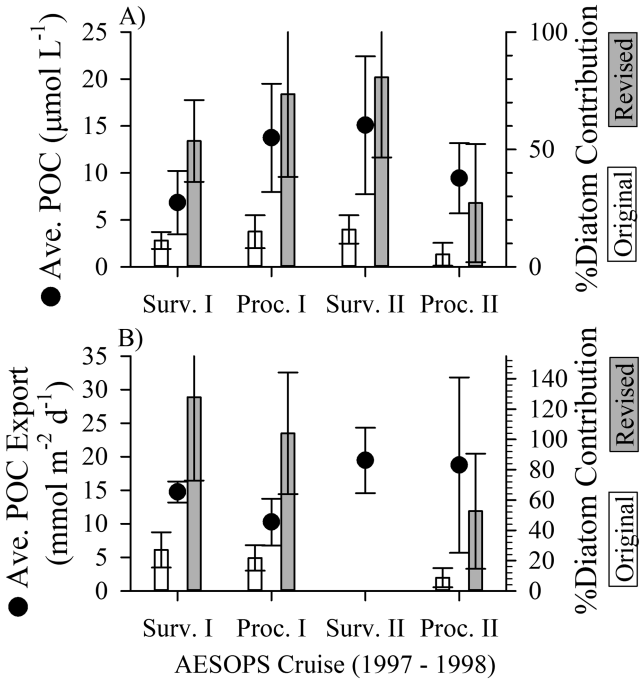

Figure 2. Reanalysis of cruise data from the Southern Ocean during the JGOFS AESOPS survey I, process I, survey II, and process II cruises (1997–1998). A cruise-averaged POC in the upper 50 m (filled circle) and the cruise-averaged diatom contribution to POC in the upper 50 m using the original temperate diatom allometry (open bars) and the contribution recalculated using cold-water diatom allometry (gray bars). B cruise-averaged thorium-derived POC export (100 m) using steady-state assumptions and the cruise-averaged diatom contribution to POC export, calculated by converting $bSiO_2$ flux to POC using the upper 50-m water column $bSiO_2$:Diatom carbon ratio, where diatom carbon was derived from temperate allometry (open bars) or cold-water allometry (gray bars). Original data accessed through www.bco-dmo.org (see section 2). Error bars are standard deviation.

3.2. Have Diatoms' Biogeochemical Importance in High-Latitude Marine Systems Been Systematically Underestimated?

We assess whether studies using temperate phytoplankton allometry to estimate diatom element-based biomass in high-latitude marine systems require revision. Using cold-water diatom allometry, we reanalyzed diatom biovolume data from the U.S. JGOFS AESOPS project. These cruises were conducted in early austral spring (October–November, Survey I), late austral spring (December, Process I), and austral summer (January, Survey II; February–March, Process II). Each cruise progressively sampled further south as the ice edge retreated. A phytoplankton bloom, dominated by diatoms, developed between the first and second cruises (austral spring), and propagated southward following the ice-edge recession (Nelson et al., 2001). Brzezinski et al. (2001) described this bloom as "intense" and the accumulation of diatom biomass (as $bSiO_2$) in the euphotic zone ranged between 150 and 800 mmol Si/m^2. This diatom $bSiO_2$ accumulation was comparable to, or exceeded, the highest euphotic-zone diatom biomass quantified in the oceans' most productive upwelling systems, for example, NW Africa, Baja California, Peru, Monterey Bay (Brzezinski et al., 2003; Goering et al., 1973; Nelson et al., 1981).

AESOPS reanalysis shows systematic underestimates in the magnitude of biovolume-derived diatom standing stock and POC contributions. Using the original temperate allometry, the average diatom contribution to total POC standing stock within the upper 50 m ranged from 5–16% among the four cruises (median contributions 4–17%, Figure 2(a)); these values did not appear to be biased low by nonbloom stations, as the standard deviation ranged from 4–7% among cruises. Indeed, summing all protozoan carbon and comparing to total POC standing stock, Landry et al. (2002) noted "protists averaged 58% of POC for all stations, a value that seems reasonable with respect to likely contributions from detritus and bacteria." Given the exceptional diatom biomass accumulation during AESOPS, it would be expected that diatoms' contribution to POC would have far exceeded the cruise averages (<20%) originally reported. Our reanalysis suggests that the cruise-averaged diatom contribution to total POC ranged between 27% and 81%; the cruise-specific median values were comparable, ranging between 15% and 89%. Additionally, increasing the diatom contribution to the total POC pool and adding the heterotrophic and nondiatom autotrophic protist contributions reported by Landry et al. (2002), increases the cruise-averaged total protist contribution from 34–87% of the total bulk POC pool among the four cruises (cruise-median values range 24–94%). These reanalysis values, based on cold-water diatom allometry, suggest that the diatom contribution to POC during the AESOPS bloom events were considerably higher than initially reported and more proportionate to the intense biomass accumulation reported by Brzezinski et al. (2001). Taken together, these findings have major implications for biogeochemical models published using the AESOPS data (Fennel et al., 2003; Moore et al., 2001) as the high proportion of diatom POC increases the perceived coupling between regional C and Si cycles. This provides compelling evidence as to why this sector of the Southern Ocean has high euphotic-zone organic-matter-export efficiency.

A similar reanalysis is required for estimating diatoms' contribution to the total $bSiO_2$ during AESOPS. When applying the temperate diatom allometry, living diatoms would have only accounted for 3–8% of the total $bSiO_2$ among cruises. Applying the cold-water diatom allometry, living diatoms would have contributed 34–115% of the total $bSiO_2$ among the four AESOPS cruises, with high variability in the Survey I cruise (115% ± 61%). During AESOPS, iron was limiting, and this decoupled Si and N uptake by diatoms (Franck et al., 2000); however, Si was also kinetically limiting at times (Nelson et al., 2001). These effects can increase (iron limitation) and decrease (kinetic limitation of Si uptake) silicification, which may

explain why the average exceeds 100% and is so variable. The other three cruises were more consistent, averaging 34–51% living diatom contribution to the total $bSiO_2$.

The increase in the proportion of living diatoms to the total $bSiO_2$ pool reconciles dilution-based (Selph et al., 2001) and silicon-tracer-based (Brzezinski et al., 2001) rates of $bSiO_2$ production during the AESOPS Process I cruise. Selph et al. (2001) reported average diatom growth rates ranging between 0.08 and 0.56 day^{-1} in the upper 25 m. Multiplying that rate by the average proportion of living diatom $bSiO_2$ derived using temperate allometry among these same stations and depth interval (i.e., upper 25 m, 0.1–0.3 μmol Si/L) yields an average $bSiO_2$ production rate of 0.09 ± 0.05 μmol $Si \cdot L^{-1} \cdot day^{-1}$; this is significantly (t test, $p < 0.001$) lower than the silicon tracer average of 0.77 ± 0.22 μmol $Si \cdot L^{-1} \cdot day^{-1}$ at the same stations and depths (Brzezinski et al., 2001). However, if we use the cold-water diatom allometry to derive living diatom $bSiO_2$ (i.e., upper 25 m, 1.5–3.2 μmol Si/L) and multiply it by the diatom growth rate range above, the average is 1.11 ± 0.56 μmol $Si \cdot L^{-1} \cdot day^{-1}$, which is not significantly different (t test, $p = 0.21$) from the directly measured rates. Applying cold-water diatom allometry to these previously published data resolves the major disparity between estimates of diatom $bSiO_2$ production based on coupled dilution-method growth rates and living diatom $bSiO_2$ versus direct silicon tracer measurements.

Given the high diatom contribution to POC during AESOPS, it is surprising that the average proportion of the total $bSiO_2$ associated with living diatoms in the reanalysis ranged 34–51% during the Process I, Survey II, and Process II cruises. Such a finding suggests there was a significant component of the total $bSiO_2$ associated with detrital $bSiO_2$ (e.g., fragments) and/or contributions from other silicifying groups (Rhizaria; Biard et al., 2018; *Synechococcus,* Baines et al., 2012). Distributions of *Synechococcus* suggest they are small contributors to POC in the poles (Buitenhuis et al., 2012). Additionally, Rhizaria contribution to particulate export during AESOPS was minor compared to diatoms (Grigorov et al., 2014), which is consistent with biomass in the upper 200 m being orders of magnitude lower in high latitudes versus lower latitudes (Biard et al., 2016). We conclude the nondiatom $bSiO_2$ in the Southern Ocean during AESOPS was predominantly detrital diatom fragments; this validates AESOPS models showing similar results (Fennel et al., 2003). During AESOPS, protist grazers consumed ~60% of daily diatom production (Selph et al., 2001); thus, protist grazing appeared to be the main process producing detrital $bSiO_2$. Low temperatures reduce the physicochemical dissolution rate for $bSiO_2$ and the rate of bacteria-mediated dissolution (Bidle et al., 2002); this coupled with high protist grazing losses for diatoms increases the residence time for detrital $bSiO_2$ in the water column until it is aggregated and exported. Such a finding is important, as bulk particulate material in this region is enriched in Si, relative to C, which affects how the diatom contribution to POC export is derived and interpreted.

Using the published export data (Buesseler et al., 2001), we revise upward the diatom contribution to POC export during AESOPS. Temperate allometric determination of diatom carbon (to determine $bSiO_2$:diatom carbon ratio) infers that diatoms only accounted for 9–27% of the POC export among AESOPS cruises (Figure 2(b)). If we use cold-water diatom allometry, which increases diatom carbon and thereby decreases the $bSiO_2$:diatom carbon ratio, then the average diatom contribution to POC export increases to 53–128% among the AESOPS cruises. If diatom detrital material gets consumed more than once in the water column, for example, zooplankton grazing on detrital aggregates or fecal pellets, then this would increase the diatom Si:C and explain why the calculated diatom contributions exceed 100%. This is supported by work during the Process I cruise (128% value, above) suggesting that fecal pellets from large copepods could have accounted for 42–107% of the $bSiO_2$ flux (Dagg et al., 2003). During the summer cruise (Process II) the fecal pellet contribution was only 1–5% of the diatom $bSiO_2$ flux (Dagg et al., 2003), and this is consistent with the reduction in the diatom contribution to 53% (Figure 2(b)). The reanalysis suggests diatoms (in various exported forms) could have accounted for a majority of POC export during the AESOPS cruises.

Beyond the AESOPS program, results from the European Iron Fertilization Experiment (EIFEX) project may also require reassessment. Assmy et al. (2013) reported that total $bSiO_2$ ranged from 400–800 mmol Si/m^2 in the surface layers (like the "intense" amount of diatom biomass reported during AESOPS), yet diatom carbon associated with the main diatom genera only increased to 50–200 mmol C/m^2. Such a range in diatom carbon is low, compared to the $bSiO_2$ magnitude, and infers that only 1–11% of the total $bSiO_2$ during the bloom was associated with living diatoms. Additionally, Assmy et al. (2013) report that most of the

diatom biomass in the surface layer was associated with intact diatoms as opposed to broken or empty valves, which seems at odds with observed stock data. The cold-water-diatom allometry and stoichiometric relationships suggest that the diatom carbon should have been enhanced by at least a factor of 6.5 (median value) over the temperate allometry values. Applying this uniformly to the EIFEX diatom data, and comparing with the quantified bulk $bSiO_2$ values, implies that 10–75% of the EIFEX $bSiO_2$ during the diatom bloom was associated with living diatoms. Like the AESOPS diatom bloom, we posit that the diatom-associated carbon was significantly underestimated during EIFEX.

Many other studies have applied temperate phytoplankton allometry (e.g., Armand et al., 2008; Cornet-Barthaux et al., 2007; Lasbleiz et al., 2016; Leblanc et al., 2012; Sherr et al., 2003) to estimate diatom carbon in both the northern and southern polar regions. Systematically assessing each is beyond our scope; however, it is notable that studies originating from the northern Kerguelen Plateau region, which has naturally iron-fertilized surface waters, appears different from ASGARD, AESOPS, and EIFEX. Specifically, in two major field programs (2005, 2011) diatom carbon was quantified using the temperate allometric relationship. Both studies demonstrated diatom biomass was, in many cases, most of the bulk POC (Armand et al., 2008; Lasbleiz et al., 2016). Additionally, when considering all plankton groups, their POC sum aligned well with bulk POC measurements (Lasbleiz et al., 2016). Applying the cold-water diatom allometry to these data result in unrealistically high diatom contributions, where they alone could exceed bulk POC measurements; thus, our hypothesis that all polar studies applying diatom allometry have systematically underestimated their abundance is disproved. The disparity and reasons for why this may be are unknown; however, it could be driven by the relatively unique biogeochemical cycling of the Kerguelen Plateau which has been described as a "natural laboratory" due to its innate and persistent iron fertilization (Lasbleiz et al., 2016). We suggest that future efforts examine more Southern Hemisphere diatom species adapted to cold water and the underlying factors regulating diatom BED for major bioactive elements (C, N, P, Si), as this is critical to accurately model their carbon flow. However, we demonstrate an alternative set of allometric equations for cold-adapted diatoms should be considered in polar studies.

3.3. Polar Diatoms in a Warming World

Given the trends of accelerated warming of SST in high latitudes, changes in cold-water diatom BED may have a significant impact on the future efficiency of trophic transfer and total carbon flow in these systems. Relative to 1986–2005, Arctic Ocean SST is projected to increase between 2° and 5° (RCP2.6 scenario) or 7–11° (RCP8.5 scenario) by 2100 (IPCC, 2014). Some researchers have suggested the resulting loss of sea ice, due to warming, may increase the area for primary productivity and the duration of the growing season (Arrigo et al., 2008) or stimulate more under-ice blooms (Arrigo et al., 2014).

Whether or not diatoms will continue to dominate spring productivity and drive the most important annual period for secondary production is questionable. Size spectrum shifts (diatoms toward smaller picoplankton) have been reported in the Canadian Arctic (Li et al., 2009). This contrasts broader studies, which show no such trend in the North Atlantic (McQuatters-Gollop et al., 2011). Increases in the total primary production projected in the future, may be driven by enhancement of other phytoplankton groups. If diatoms can maintain the status quo for carbon BED and their absolute quantity of production in a warming ocean, such shifts may proportionally reduce diatoms' contribution to the community rates but might not have an adverse effect on trophic coupling. However, we hypothesize that increased warming in the polar regions will reduce diatom carbon BED and therefore reduce their transferred carbon.

We derive a Q_{10} metric to examine how diatom BED could change with increasing polar zone SST. A widely used temperate diatom carbon BED is 0.3 pg C/μm^3 derived from clones grown between 10 °C and 20 °C (Menden-Deuer & Lessard, 2000, and references therein). The cold-water diatom carbon BED (2 °C) ranged from 1.3 pg C/μm^3 (stationary growth) to 1.6 pg C/μm^3 (exponential growth; Lomas et al., 2019). Given that elemental content and biovolume relationships are logarithmic and that we only have BED data for two thermal conditions (i.e., 2 and 10–20 °C), we modify a Q_{10} approach to make a first-order estimate on how BED changes as a function of temperature. Our analysis suggests the diatom carbon BED Q_{10} ranges between 0.25 and 0.40.

Given IPCC scenarios for the Arctic, significant changes to diatom BED may occur with increasing SST (Figure 3). For SST increases <2 °C, the reduction in diatom carbon BED is <0.38 pg C/μm^3; this change

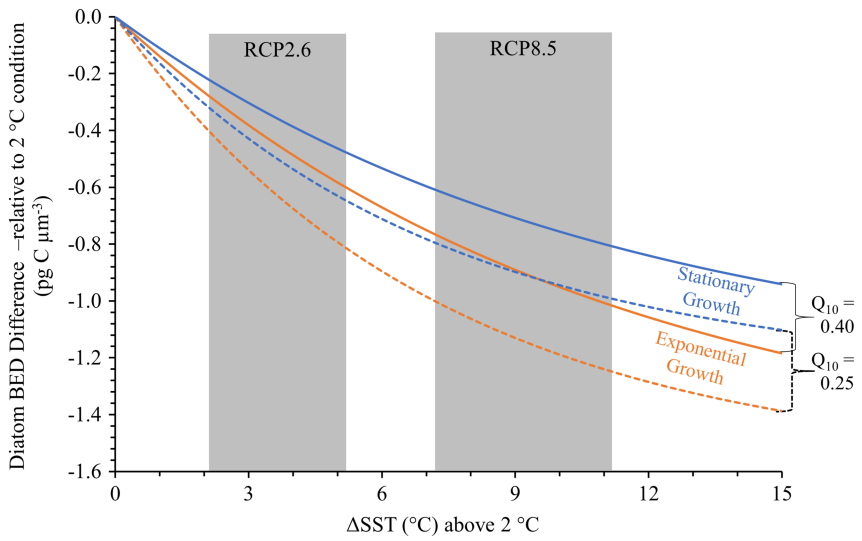

Figure 3. Predicted decline in cold-water diatom carbon BED, relative to that at 2 °C, with increasing SST in the cold-water environments. Highlighted ranges show two IPCC-predicted scenarios (RCP2.6 and RCP8.5) where Arctic SST increases at the end of the 21st century, relative to 1986–2005. Trajectories include a range of diatom carbon BED Q_{10} estimates (0.25, dashed line; 0.40, solid line) and whether diatoms are growing in stationary (blue) or exponential (orange) phases.

is the same order of magnitude as the temperate diatom carbon BED. Under the conservative RCP2.6 scenario, the diatom carbon BED is predicted to decline by 0.21–0.79 pg C/µm^3. Under the liberal RCP8.5 scenario, the diatom carbon BED is predicted to reduce by 0.60–1.24 pg C/µm^3. Thus, in the best-case forecast, diatom carbon BED would reduce by 50%, relative to current levels, while the worst-case scenario would result in their carbon BED converging with temperate diatoms.

If cold-water diatom carbon BED were similar to that of temperate diatoms, we would expect major food web shifts. For instance, reduction in diatom carbon BED could reduce the diatom elemental quality per cell for grazers (copepods, krill). Such a decline in prey quality could be compensated by grazers consuming more diatoms (e.g., Frost, 1972), but there would be a metabolic cost to added foraging. Therefore, it is likely that polar food web trophic-transfer efficiency between primary producers and primary consumers would be reduced with a thermally driven decline in diatom carbon BED.

Predicting the role of diatoms in primary production in a warming ocean is important to understand potential effects for higher trophic levels (e.g., fisheries). The ideas presented here are consistent with model simulations suggesting that diatom contribution to primary production will decline everywhere outside of the Southern Ocean in the future (Tréguer et al., 2018). However, these authors also suggest a strong role for diatom species to shift in response to climate. The scenarios we examine, especially RCP2.6, may not result in a SST increase intense enough to fully favor species succession and may just foster local adaptation. However, our analysis suggests that increasing SST could play a strong role in reducing diatom BED and therefore, alter the fate of diatom organic matter in the food web even without major changes in diatom community composition. Clearly, we still require more foundational information before accurately predicting diatoms' responses to increasing warming; however, we argue that the fundamental role of temperature in high-latitude regions, which are warming at an accelerated rate, must be explored in more detail (e.g., beyond temperature effects on growth rates) to accurately model the response in the food web and secondary production.

Acknowledgments
Funding was provided by the National Science Foundation Office of Polar Programs (OCE-1603605, J, K.; OCE-1603460, M. L.) and logistic and vessel support by the North Pacific Research Board (NA15NMF4720173 to M. L., subaward to J. K.). We thank ASGARD Chief Scientist S. Danielson, along with the science party and crew including marine technicians S. Hartz and E. Roth; D. Wiik, T. Martinson, and D. Harlan for logistical support, S. Acton and W. Dobbins for laboratory support, M. Stukel for insightful discussion, and two anonymous reviewers for providing constructive comments. The original project data are available as supporting information and at the National Science Foundation Arctic Data Center (doi:10.18739/A2SF2MC1D). Reanalysis data are provided in the supporting information, and original AESOPS data can be accessed through the Biological and Chemical Oceanography Data Management Office (www.bco-dmo.org/project/2044).

References

Armand, L. K., Cornet-Barthaux, V., Mosseri, J., & Queguiner, B. (2008). Late summer diatom biomass and community structure on and around the naturally iron-fertilised Kerguelen plateau in the Southern Ocean. *Deep Sea Research Part II: Topical Studies in Oceanography*, *55*(5–7), 653–676.

Arrigo, K. R., Perovich, D. K., Pickart, R. S., Brown, Z. W., van Dijken, G. L., Lowry, K. E., et al. (2014). Phytoplankton blooms beneath the sea ice in the Chukchi Sea. *Deep Sea Research Part II: Topical Studies in Oceanography*, *105*, 1–16.

Arrigo, K. R., van Dijken, G., & Pabi, S. (2008). Impact of a shrinking Arctic ice cover on marine primary production. *Geophysical Research Letters*, *35*, L19603. https://doi.org/10.1029/2008GL035028

Assmy, P., Smetacek, V., Montresor, M., Klaas, C., Henjes, J., Strass, V. H., et al. (2013). Thick-shelled, grazer-protected diatoms decouple ocean carbon and silicon cycles in the iron-limited Antarctic circumpolar current. *Proceedings of the National Academy of Sciences*, *110* (51), 20,633–20,638.

Baines, S. B., Twining, B. S., Brzezinski, M. A., Krause, J. W., Vogt, S., Assael, D., & McDaniel, H. (2012). Significant silicon accumulation by marine picocyanobacteria. *Nature Geoscience*, *5*, 886–891.

Biard, T., Krause, J. W., Stukel, M. R., & Ohman, M. D. (2018). The significance of giant phaeodarians (rhizaria) to biogenic silica export in the California current ecosystem. *Global Biogeochemical Cycles*, *32*, 987–1004. https://doi.org/10.1029/2018GB005877

Biard, T., Stemmann, L., Picheral, M., Mayot, N., Vandromme, P., Hauss, H., et al. (2016). In situ imaging reveals the biomass of giant protists in the global ocean. *Nature*, *532*(7600), 504–507. https://doi.org/10.1038/nature17652

Bidle, K. D., Manganelli, M., & Azam, F. (2002). Regulation of oceanic silicon and carbon preservation by temperature control on bacteria. *Science*, *298*(5600), 1980–1984. https://doi.org/10.1126/science.1076076

Brown, S. L., & Landry, M. R. (2001). Microbial community structure and biomass in surface waters during a polar front summer bloom along 170 W. *Deep Sea Research Part II: Topical Studies in Oceanography*, *48*(19–20), 4039–4058.

Brzezinski, M. A., Jones, J. L., Bidle, K. D., & Azam, F. (2003). The balance between silica production and silica dissolution in the sea: Insights from Monterey Bay, California, applied to the global data set. *Limnology and Oceanography*, *48*(5), 1846–1854.

Brzezinski, M. A., Nelson, D. M., Franck, V. M., & Sigmon, D. E. (2001). Silicon dynamics within an intense open-ocean diatom bloom in the Pacific sector of the Southern Ocean. *Deep Sea Research, Part II*, *48*(19–20), 3997–4018.

Buesseler, K., Ball, L., Andrews, J., Cochran, J., Hirschberg, D., Bacon, M., et al. (2001). Upper Ocean export of particulate organic carbon and biogenic silica in the Southern Ocean along 170 W. *Deep Sea Research Part II: Topical Studies in Oceanography*, *48*(19–20), 4275–4297.

Buitenhuis, E. T., Li, W. K. W., Vaulot, D., Lomas, M. W., Landry, M. R., Partensky, F., et al. (2012). Picophytoplankton biomass distribution in the global ocean. *Earth System Science Data*, *4*(1), 37–46. https://doi.org/10.5194/essd-4-37-2012

Conley, D. J., Kilham, S. S., & Theriot, E. (1989). Differences in silica content between marine and fresh-water diatoms. *Limnology and Oceanography*, *34*(1), 205–213.

Cornet-Barthaux, V., Armand, L., & Quéguiner, B. (2007). Biovolume and biomass estimates of key diatoms in the Southern Ocean. *Aquatic Microbial Ecology*, *48*(3), 295–308.

Dagg, M. J., Urban-Rich, J., & Peterson, J. O. (2003). The potential contribution of fecal pellets from large copepods to the flux of biogenic silica and particulate organic carbon in the Antarctic polar front region near 170 W. *Deep Sea Research, Part II*, *50*(3), 675–691.

Eppley, R. W. (1972). Temperature and phytoplankton growth in the sea. *Fishery Bulletin*, *70*(4), 1063–1085.

Eppley, R. W., Reid, F. M. H., & Strickland, J. D. H. (1970). Estimates of phytoplankton crop size, growth rate, and primary production. In J. D. H. Strickland (Ed.), *The Ecology of Plankton off La Jolla California in the Period April through September, 1967*, (pp. 33–42). La Jolla, California: University of California Press.

Fennel, K., Abbott, M. R., Spitz, Y. H., Richman, J. G., & Nelson, D. M. (2003). Modeling controls of phytoplankton production in the Southwest Pacific sector of the Southern Ocean. *Deep-Sea Research Part II-Topical Studies in Oceanography*, *50*(3–4), 769–798.

Franck, V. M., Brzezinski, M. A., Coale, K. H., & Nelson, D. M. (2000). Iron and silicic acid concentrations regulate Si uptake north and south of the polar frontal zone in the Pacific sector of the Southern Ocean. *Deep Sea Research, Part II*, *47*(15–16), 3315–3338.

Frost, B. (1972). Effects of size and concentration of food particles on the feeding behavior of the marine planktonic copepod *Calanus Pacificus*. *Limnology and Oceanography*, *17*(6), 805–815.

Goering, J. J., Nelson, D. M., & Carter, J. A. (1973). Silicic acid uptake by natural populations of marine phytoplankton. *Deep Sea Research*, *20*(9), 777–789.

Grigorov, I., Rigual-Hernandez, A. S., Honjo, S., Kemp, A. E., & Armand, L. K. (2014). Settling fluxes of diatoms to the interior of the Antarctic circumpolar current along 170 W. *Deep Sea Research Part I: Oceanographic Research Papers*, *93*, 1–13.

IPCC (2014). *Climate change 2014: Synthesis Report. Rep*, (p. 151). Geneva, Switzerland: IPCC.

Krause, J. W., Brzezinski, M. A., Goericke, R., Landry, M. R., Ohman, M. D., Stukel, M. R., & Taylor, A. G. (2015). Variability in Diatom Contributions to Biomass, Organic Matter Production, and Export across a Frontal Gradient in the California Current Ecosystem. *Journal of Geophysical Research: Oceans*, *120*, 1032–1047. https://doi.org/10.1002/2014JC010472

Krause, J. W., Brzezinski, M. A., & Jones, J. L. (2011). Application of low level beta counting of 32Si for the measurement of silica production rates in aquatic environments. *Marine Chemistry*, *127*, 40–47.

Krause, J. W., Brzezinski, M. A., Landry, M. R., Baines, S. B., Nelson, D. M., Selph, K. E., et al. (2010). The effects of biogenic silica detritus, zooplankton grazing, and diatom size structure on silicon cycling in the euphotic zone of the eastern equatorial Pacific. *Limnology and Oceanography*, *55*(6), 2608–2622.

Krause, J. W., Nelson, D. M., & Lomas, M. W. (2009). Biogeochemical responses to late-winter storms in the Sargasso Sea, II: Increased rates of biogenic silica production and export. *Deep Sea Research, Part I*, *56*(6), 861–874.

Kremer, C. T., Thomas, M. K., & Litchman, E. (2017). Temperature-and size-scaling of phytoplankton population growth rates: Reconciling the Eppley curve and the metabolic theory of ecology. *Limnology and Oceanography*, *62*(4), 1658–1670.

Landry, M. R., Selph, K. E., Brown, S. L., Abbott, M. R., Measures, C. I., Vink, S., et al. (2002). Seasonal dynamics of phytoplankton in the Antarctic polar front region at 170° W. *Deep Sea Research Part II: Topical Studies in Oceanography*, *49*(9–10), 1843–1865.

Lasbleiz, M., Leblanc, K., Armand, L. K., Christaki, U., Georges, C., Obernosterer, I., & Quéguiner, B. (2016). Composition of diatom communities and their contribution to plankton biomass in the naturally iron-fertilized region of Kerguelen in the Southern Ocean. *FEMS Microbiology Ecology*, *92*(11), fiw171.

Leblanc, K., Arístegui, J., Kopczynska, E., Marshall, H., Peloquin, J., Piontkovski, S., et al. (2012). A global diatom database–abundance, biovolume and biomass in the world ocean. *Earth System Science Data*, *5*(1), 147–185.

Li, W. K., McLaughlin, F. A., Lovejoy, C., & Carmack, E. C. (2009). Smallest algae thrive as the Arctic Ocean freshens. *Science*, *326*(5952), 539–539. https://doi.org/10.1126/science.1179798

Lomas, M. W., S. E. Baer, S. Acton, And J. W. Krause (2019), pumped up by the cold: Elemental quotas and stoichiometry of polar diatoms, *Frontiers in Marine Science*, *6*, DOI: https://doi.org/10.3389/fmars.2019.00286

McQuatters-Gollop, A., Reid, P. C., Edwards, M., Burkill, P. H., Castellani, C., Batten, S., et al. (2011). Is there a decline in marine phytoplankton? *Nature*, *472*(7342), E6.

Menden-Deuer, S., & Lessard, E. J. (2000). Carbon to volume relationships for dinoflagellates, diatoms, and other protist plankton. *Limnology and Oceanography*, *45*(3), 569–579.

Moore, J. K., Doney, S. C., Kleypas, J. A., Glover, D. M., & Fung, I. Y. (2001). An intermediate complexity marine ecosystem model for the global domain. *Deep Sea Research Part II: Topical Studies in Oceanography*, *49*(1–3), 403–462.

Nelson, D. M., Brzezinski, M. A., Sigmon, D. E., & Franck, V. M. (2001). A seasonal progression of Si limitation in the Pacific sector of the Southern Ocean. *Deep Sea Research, Part II*, *48*(19–20), 3973–3995.

Nelson, D. M., J. J. Goering, And D. W. Boisseau (1981), consumption and regeneration of silicic acid in three coastal upwelling systems, in *Coastal Upwelling*, edited by F. A. Richards, pp. 242-256, American Geophysical Union Washington D. C.

Selph, K. E., Landry, M. R., Allen, C. B., Calbet, A., Christensen, S., & Bidigare, R. R. (2001). Microbial community composition and growth dynamics in the Antarctic polar front and seasonal ice zone during late spring 1997. *Deep Sea Research, Part II*, *48*(19–20), 4059–4080.

Sherr, E. B., Sherr, B. F., Wheeler, P. A., & Thompson, K. (2003). Temporal and spatial variation in stocks of autotrophic and heterotrophic microbes in the upper water column of the Central Arctic Ocean. *Deep Sea Research Part I: Oceanographic Research Papers*, *50*(5), 557–571.

Smith, W. O., Anderson, R. F., Moore, J. K., Codispoti, L. A., & Morrison, J. M. (2000). The US southern ocean joint global ocean flux study: An introduction to AESOPS. *Deep Sea Research Part II: Topical Studies in Oceanography*, *47*(15–16), 3073–3093.

Takeda, S. (1998). Influence of iron availability on nutrient consumption ratio of diatoms in oceanic waters. *Nature*, *393*(6687), 774–777.

Tréguer, P., Bowler, C., Moriceau, B., Dutkiewicz, S., Gehlen, M., Aumont, O., et al. (2018). Influence of diatom diversity on the ocean biological carbon pump. *Nature Geoscience*, *11*(1), 27.

Tremblay, J.-E., Gratton, Y., Fauchot, J., & Price, N. M. (2002). Climatic and oceanic forcing of new, net, and diatom production in the north water. *Deep Sea Research Part II: Topical Studies in Oceanography*, *49*(22–23), 4927–4946.